

# Articles

## Morphologies and Growth Model of Biomimetic Fabricated Calcite Crystals Using Amino Acids and Insoluble Matrix Membranes of *Mytilus edulis*

Wen-Tao Hou and Qing-Ling Feng\*

Department of Materials Science and Engineering, Laboratory of Advanced Materials, Tsinghua University, Beijing 100084, People's Republic of China

Received September 22, 2005; Revised Manuscript Received March 1, 2006

**ABSTRACT:** Protein membranes extracted from mollusk shells were selected as substrates to precipitate calcium carbonate crystals in  $\text{CaCl}_2$  solutions containing glycine or aspartic acid. This research mainly concentrated on the morphologies of the synthesized calcite particles rather than on the control over the polymorphs. The amino acids might restrict the growth of the negative directions of the calcite's  $\{104\}$  faces. Aspartic acid might serve as an agglutinant of several crystals. Compared with the silicon substrate results, protein membranes of the nacreous layer have obvious inductivity of nucleation through interfacial matching to the (001) faces of calcite crystals, and in the presence of glycine we also observed some mushroom-like particles. Their nucleation orientation and formation mechanism were represented by schematics. On the other hand, protein membranes of the prismatic layer did not have similar functions. These works are in vitro studies of biomineralization.

### 1. Introduction

Calcium carbonate is one of the most ubiquitous minerals in nature and is also widely found as biominerals in various species, especially mollusks. There are three important polymorphs of calcium carbonate: calcite, aragonite, and vaterite (metastable form). Their crystal lattices are rhombohedral, orthorhombic, and hexagonal, respectively.<sup>1</sup> Much research has been reported on their thermodynamics and growth kinetics.<sup>2,3</sup>

In mollusk shells, inorganic components are dominant with over 95% of the mass or volume. Those in the prismatic layer are (001)-oriented calcite crystals, and those in the nacreous layer are *c*-axis-oriented aragonite tablets.<sup>4</sup> The organic matrix is composed of  $\beta$ -chitin, silk-fibroin-like proteins, and acidic macromolecules in the interlaminar space between crystals.<sup>5</sup> On the basis of the solubility in sodium ethylenediaminetetraacetic acid (EDTA), they are classified as insoluble matrix (IM) proteins and soluble matrix (SM) proteins. In one of our previous studies, IM and SM are found to have different roles in polymorph and morphology control of calcium carbonate.<sup>6</sup> Amino acid analysis of SM found that the three most important amino acids are glycine (Gly), aspartic acid (Asp), and glutamic acid (Glu).<sup>7,8</sup> That is why we choose Gly and Asp as additives in calcite synthesis. The above research concentrated either on structure and orientation of crystals in mollusk shells or on polymorphs of SM/IM induced calcium carbonate. In this paper, we mimicked the biomineralization process to fabricate calcite

crystals but mainly to analyze morphologies and orientation relationships.

Atomic force microscope (AFM) studies of calcite growth in low-saturation solutions showed distinct images of spiral growth hillocks and step advance.<sup>9,10</sup> And, in the presence of some additives, the hillocks might also be contrasted to analyze the influence of the additives.<sup>11,12</sup> We also used this instrument to observe organic–inorganic interfacial adsorptions and the effects of additives in our experimental environment.

### 2. Methods

The experiments were held in a closed desiccator for 24 h at 25 °C. Calcium carbonate crystals were precipitated in cell-culture dishes containing 10 mM  $\text{CaCl}_2$  solutions. After Gly or Asp were added, the pH values of the solutions were adjusted to around 5 using NaOH solution.  $\text{CO}_2$  vapor was produced by volatilization of  $\text{NH}_4\text{HCO}_3$  solid.  $\text{H}_2\text{SO}_4$  solution was also placed in the desiccator to sorb  $\text{NH}_3$  vapor.

Three sorts of substrates were used in the precipitation: silicon slips with a (100) face, calcite crystals with  $\{104\}$  cleavage planes, and IM membranes of a 2-year-old bivalve, *Mytilus edulis*. These protein membranes were obtained from nacreous or prismatic layers of mollusk shells after being decalcified in 10 wt % EDTA solution for several days. Then they were dipped in deionized water and washed for calcium carbonate synthesis. Observations were performed using a scanning electron microscope (SEM, JSM-6460LV).

Calcite substrate was put into the desiccator for only 20 min. Picoscan AFM (Molecular Imaging Co., Arizona) imaging was then performed to observe the surface hillocks with Contact Mode.

### 3. Results and Discussion

The reason for selecting silicon rather than glass cover slips as the substrate is that we found that the glass surface may

\* Corresponding author. Tel.: +86-10-62782770. Fax: +86-10-62771160. E-mail: biomater@mail.tsinghua.edu.cn.

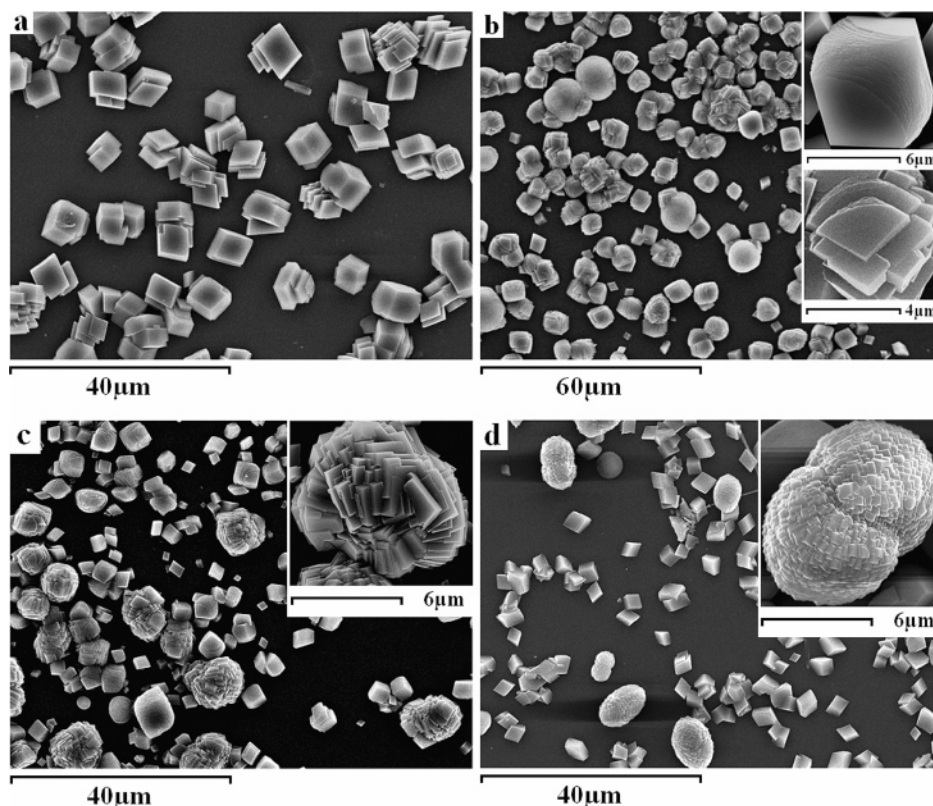


**Figure 1.** SEM morphologies of calcite crystals deposited on the silicon clips. (a) Without any additives, regular rhombohedral shape; (b) after adding 1 mM glycine, irregular at negative directions, small insets showed two kinds of morphologies; (c) after adding 1 mM aspartic acid, agglomerating appearance; (d) after adding 10 mM aspartic acid, elaborative agglomerating appearance.

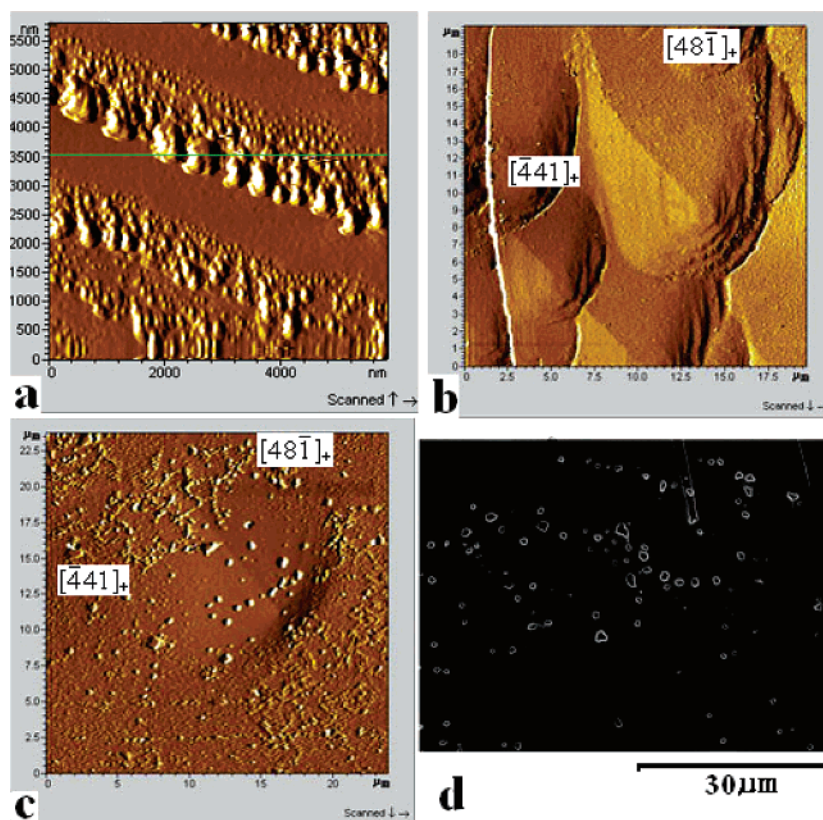


**Figure 2.** AFM images of (a) Gly adsorption on calcite cleavage steps; (b) spiral growth hillocks on the {104} face of calcite in 1 mM  $\text{CaCl}_2$  solution,  $[441]_+$  and  $[481]_+$  step edge advanced faster than  $[441]_-$  and  $[481]_-$ ; (c) a hillock in 1 mM  $\text{CaCl}_2$  solution containing 1 mM Gly,  $[441]_-$  and  $[481]_-$  completely terminated. (d) SEM image of sample (c); there are many notches produced by Gly adsorption on the surface.

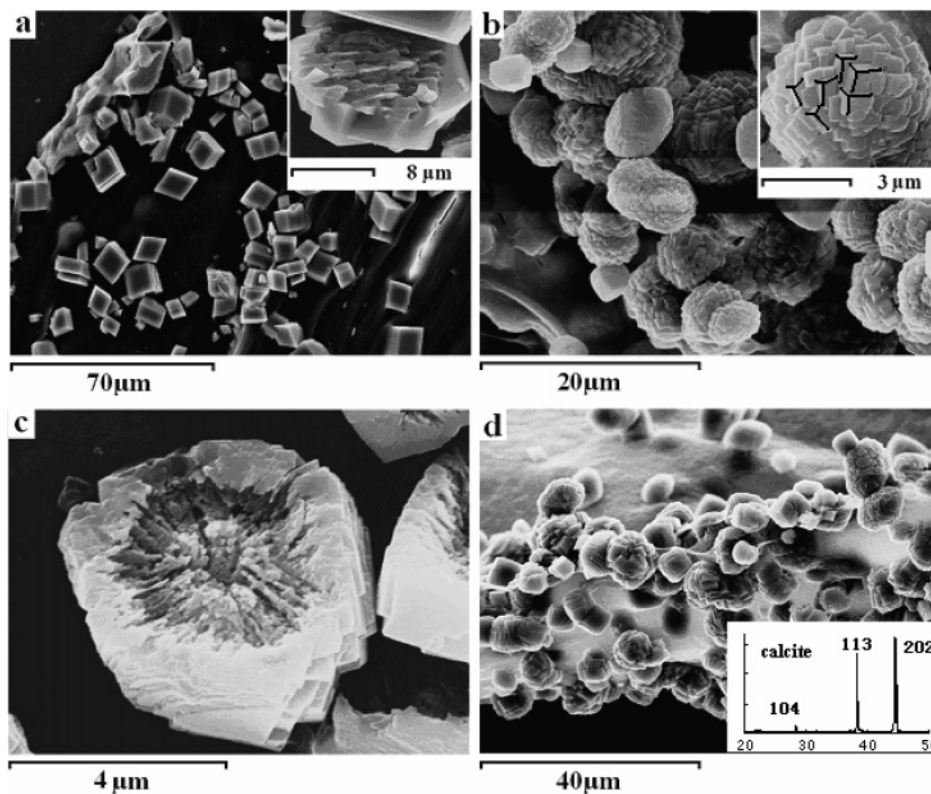


**Figure 3.** SEM morphologies of calcite crystals grown from the edge of IM membranes of the nacreous layer. (a) Without any additives, regular rhombohedral shape, inset showed a reversed block; (b) after adding 1 mM glycine, mostly aggregating appearance; in the inset, lines show six obtuse triangular pyramids; the three ones on the left are mirror symmetrical with the three ones on the right; (c) after adding 1 mM glycine, a reversed particle; (d) after adding 1 mM aspartic acid, most crystals in the edge; XRD curve is in the inset.

induce aragonite crystals.<sup>13</sup> Gly and Asp may also induce vaterite crystal formation as reported,<sup>14</sup> so we set very low solution heights to avoid formation of aragonite and vaterite. The results are shown in Figure 1. Gly restricted the growth of the negative directions of  $[441]$  and  $[48\bar{1}]$  and extruded the positive directions as an obtuse triangular pyramid of the  $\{104\}$  faces (upper inset in Figure 1b). Numbers of steps of the crystal particles also increased as shown in the lower inset in Figure 1b. In the presence of Asp, besides the two kinds of morphologies such as that in the presence of Gly, some crystal particles also have an agglomerating appearance (Figure 1c), which was caused by polynuclear growth. The nuclei were agglutinated by the surface adsorbed Asp molecules and grew together as a particle without uniform crystal orientation. So, under higher Asp concentration, the agglomerating appearance became more elaborate (Figure 1d).

AFM images showed the effects of Gly and Asp on calcite growth in detail. There are many cleavage step edges of several nanometers in height on the calcite sample surface. Gly adsorbs specifically on these edges after air-drying of a solution drop (Figure 2a). Figure 2b shows a spiral growth hillock with a height of about 10 nm. The two positive directions advanced faster than the two negative directions.<sup>15</sup> In Figure 2c, Gly completely terminates the negative directions of spiral growth, partly stops step edge advancement, and as a result makes many notches (Figure 2d), which do not exist under low supersaturation.<sup>12</sup> Asp has similar effects as Gly (AFM images not shown). These images demonstrate their inhibitory functions on calcite growth.

The adsorption of amino acid molecules on calcite is due to the electronegativity of carboxyl groups ( $-\text{COO}^-$ ). It has a similar stereochemical structure to the  $\text{C}-\text{O}_3$  triangle in the calcite crystal lattice and may especially bind surface  $\text{Ca}^{2+}$  ions

to terminate mineral growth.<sup>12</sup> In water, carboxyl groups are also inclined to bind  $-\text{NH}_3^+$  groups of another amino acid molecule. The difference between Gly and Asp is that Asp is an acidic amino acid that has two  $-\text{COO}^-$  groups in one molecule. This is a possible reason that Asp has the ability of agglutinating two or more nuclei, but Gly does not seem to have this ability.

In many reports and in our previous research, IM were either extracted from powders of mollusk shells or extracted as membranes and the induced precipitations were isolated for characterization.<sup>6,16,17</sup> These methods could not show the original relationship between organic and inorganic orientations as in vivo. Improved methods in the present research used pieces of the shells to extract IM membranes with sizes of about several millimeters. After synthesis of calcium carbonate, the membranes were directly observed by SEM with precipitations on them.

In using IM membranes of the nacreous layer as substrates, most crystals were distributed at the edge of the membrane surface. The calcite density was much higher than that on the midland (Figure 3d). The possible reason is that broken edge of the membrane has more active functional groups to induce calcite nucleation.

Without any additives, the precipitated crystals are regular calcite particles. The inset in Figure 3a shows a reversed calcite particle with a dentiform interface, which was caused by growth along the membrane. This particle is made of several crystals, and their  $c$ -axes are approximately perpendicular to the interface (Figure 4a). This implies that the particle grows from several membrane-induced nuclei through (001) face matching. Weiner et al. found that the antiparallel  $\beta$ -pleated sheet in the matrix of mollusk shells has Asp-X-Asp structures (X is a neutral residue).<sup>5,18</sup> This periodic structure may bind  $\text{Ca}^{2+}$  ions to form

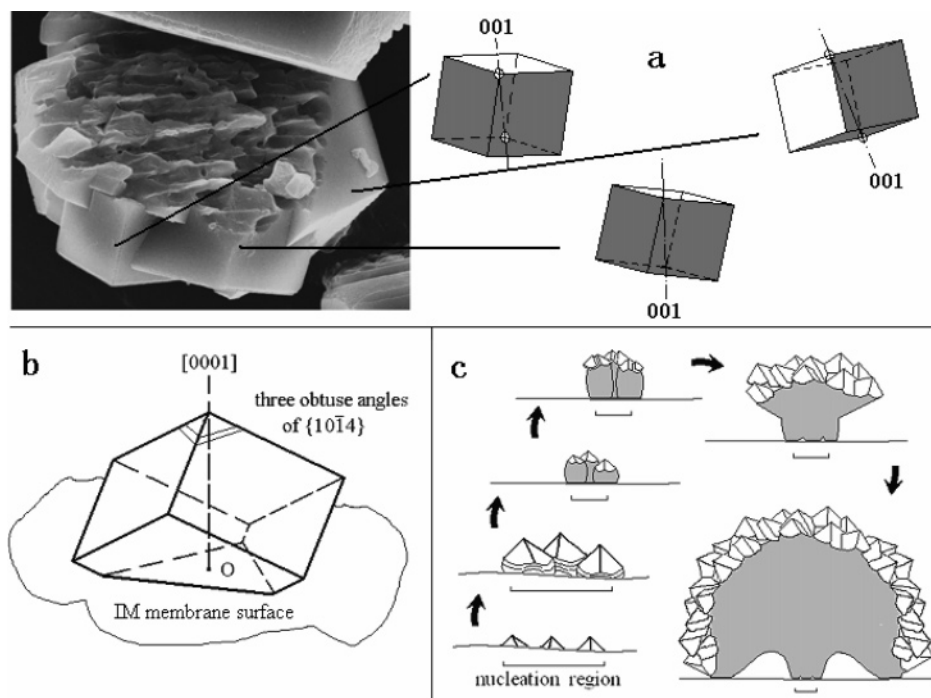


**Figure 4.** (a) Crystal orientation analysis of Figure 3a; their [001] directions are approximately perpendicular to the interface. (b) A nucleus formed on the IM membrane with its (001) face matched to the surface. After growth, its vertex of the three obtuse angles of the {104} faces is on the top position. (c) Schematic illustration of crystal growth in the presence of Gly. The underlines represent the nucleation region on the membrane, and the gray area represents bulks of the particle.

(001) faces of calcite or aragonite crystals.<sup>19–21</sup> Our observations suggest similar structural correspondence between the membrane and the fabricated calcite crystals. In Figure 4b, a schematic representation showed the process of crystal formation. It nucleates at O point and grows with its [001] direction perpendicular to the membrane surface. When several crystals nucleate in the adjacent region, they may grow together into a particle as shown in Figure 4a.

In the presence of Gly, the aggregated orbicular particles are composed of many little pyramids of calcite (Figure 3b). Their axes of the three {104} planes, [001] directions, all seemed to be able to extend to the center of the sphere. In Figure 3c, a reversed block also shows an emissive interface with higher middle and edge parts, implying an origin in the center. The formation model of aggregated orbicular particles is shown in Figure 4c according to the interfacial inductivity and effect of Gly in AFM results.

First, calcite crystals nucleate in an inductive region of the membrane. These nuclei have the same [001] directions as in Figure 4b. However, according to the matching model, their [100] or [010] directions may be the same or have an angle of 60 degrees as calcite belongs to a hexagonal system. In macro-observation, it means that the arrangement of the obtuse triangular pyramids in the orbicular particle will be either the same or mirror symmetrical (inset in Figure 3b). The presumption is practically accurate except a little offset related to the orientation offset of the bioassembled membrane proteins or interfacial matching. The shapes of the nuclei are like the upper inset in Figure 1b (negative steps terminated). Then, because the Gly terminated region is hard to advance, further growth favors the triangular pyramids faces as bases to develop transversely (like the lower inset in Figure 1b). As a result, the particle finally grows into a “mushroom” with some hollow parts inside.

The crystals in the presence of Asp are similar to those in the presence of Gly but exhibit more diversiform and random shapes (Figure 3d). The reason is the cooperative effects of

nucleation inductivity of the membrane and the agglutinative property of Asp. So, the synthesized particles do not have obvious orientation coherence in crystallography.

Finally, we used IM membranes of the prismatic layer as a substrate. The results are identical to those using silicon slips (figure not shown). We did not find any experimental evidence of nucleation inductivity of prismatic proteins, either at the edge or on the midland. Actually, researchers believe that it is the periostracum of mollusk shells rather than the proteins in the prismatic layer that induces calcite crystals *in vivo*.<sup>4</sup>

According to the above discussion, it seems that Asp has two completely opposite functions: its  $-\text{COO}^-$  groups sometimes promote but sometimes terminate formation of calcite. The reason is easy to explain from the point of view of the attraction between  $-\text{COO}^-$  and  $\text{Ca}^{2+}$ . In the nucleation stage,  $-\text{COO}^-$  side-groups of the Asp residue in IM membranes bind  $\text{Ca}^{2+}$  ions and form a two-dimensional full-calcium face, (001)Ca of calcite or aragonite.<sup>19</sup> In the growth stage,  $-\text{COO}^-$  groups of Asp mono molecules also bind  $\text{Ca}^{2+}$  in the calcite crystal surface and prevent queued  $\text{CO}_3^{2-}$ . So, in analyzing the effects of  $-\text{COO}^-$  groups on the kinetics of calcite, it is important to pay attention to its existing state.

Comparing these *in vitro* studies with the *in vivo* formation mechanism of calcite and aragonite in mollusk shells, we also find many other connotative issues. For example, there may be a structural relationship at the prismatic–nacreous transition region from the calcite to the organic matrix and to aragonite. These problems are all valuable to investigate and may give us a more profound understanding of the biomineralization mechanism to apply in fabricating bioinspired materials.

#### 4. Conclusion

In aqueous solutions, Gly and Asp may change the shapes of calcite crystals; their negative step edges of {104} faces are terminated and curved, and the step number also increases. Asp

may agglutinate several synthesized calcite crystals and induce agglomerating morphologies.

EDTA-insoluble protein membranes extracted from the nacreous layer of mollusk shells (*M. edulis*) may promote nucleation through structural matching with (001) faces of calcite. And, in the presence of Gly, the precipitated crystals have mushroom-like shapes.

IM membranes extracted from the prismatic layer of mollusk shells (*M. edulis*) do not have organic–inorganic inductivity.

**Acknowledgment.** This work is supported by Project 50272035 of National Natural Science Foundation of China.

### References

- (1) De Leeuw, N. H.; Parker, S. C. Surface structure and morphology of calcium carbonate polymorphs calcite, aragonite, and vaterite: an atomistic approach. *J. Phys. Chem. B* **1998**, *102*, 2914–22.
- (2) Nillson, O.; Sternbeck, J. A mechanistic model for calcite crystal growth using surface speciation. *Geochim. Cosmochim. Acta* **1999**, *63*, 217–225.
- (3) Gutjahr, A.; Dabringhaus, H.; Lacmann, R. Studies of the growth and dissolution kinetics of the CaCO<sub>3</sub> polymorphs calcite and aragonite. *J. Cryst. Growth* **1996**, *158*, 296–309.
- (4) Zaremba, C. M.; Belcher, A. M.; Fritz, M.; Li, Y. L.; Mann, S.; Hansma, P. K.; Morse, D. E.; Speck, J. S.; Stucky, G. D. Critical transitions in the biofabrication of abalone shells and flat pearls. *Chem. Mater.* **1996**, *8*, 679–690.
- (5) Weiner, S.; Traub, W. Macromolecules in mollusk shells and their functions in biomineralization. *Philos. Trans. R. Soc. London B* **1984**, *304*, 425–434.
- (6) Feng, Q. L.; Pu, G.; Pei, Y.; Cui, F. Z.; Li, H. D.; Kim, T. N. Polymorph and morphology of calcium carbonate crystals induced by proteins extracted from mollusk shell. *J. Cryst. Growth* **2000**, *216*, 459–465.
- (7) Lavi, Y.; Albeck, S.; Brack, A.; Weiner, S.; Addadi, L. Control over aragonite crystal nucleation and growth: an in vitro study of biomineralization. *Chem. Eur. J.* **1998**, *4*, 389–396.
- (8) Jiang, Y.; Liu, K. W.; Liu, X. W.; Min, L. E.; Shi, A. J.; Qiu, A. D.; Li, J.; Sun, Q. Z. Analysis of protein, amino acids and some elements in mantellum of four kinds of freshwater mussel. *Nat. Prod. Res. Dev.* **2002**, *14*, 45–49.
- (9) Rachlin, A. L.; Henderson, G. S. An atomic force microscope (AFM) study of the calcite cleavage plane: image averaging in Fourier space. *Am. Mineral.* **1992**, *77*, 904–910.
- (10) Teng, H. H.; Dove, P. M.; De Yoreo, J. J. Kinetics of calcite growth: surface processes and relationships to macroscopic rate laws. *Geochim. Cosmochim. Acta* **2000**, *64*, 2255–2266.
- (11) Davis, K. J.; Dove, P. M.; De Yoreo, J. J. The role of Mg<sup>2+</sup> as an impurity in calcite growth. *Science* **2000**, *290*, 1134–1137.
- (12) Orme, C. A.; Noy, A.; Wierzbicki, A.; McBride, M. T.; Grantham, M.; Teng, H. H.; Dove, P. M.; DeYoreo, J. J. Formation of chiral morphologies through selective binding of amino acids to calcite surface steps. *Nature* **2001**, *411*, 775–779.
- (13) Hou, W. T.; Feng, Q. L. A simple method to control the polymorphs of calcium carbonate in CO<sub>2</sub>-diffusion precipitation. *J. Cryst. Growth* **2005**, *282*, 214–219.
- (14) Tong, H.; Ma, W. T.; Wang, L. L.; Wan, P.; Hu, J. M.; Cao, L. X. Control over the crystal phase, shape, size and aggregation of calcium carbonate via a L-aspartic acid inducing process. *Biomaterials* **2004**, *25*, 3923–3929.
- (15) Teng, H. H.; Dove, P. M.; De Yoreo, J. J. Reversed calcite morphologies induced by microscopic growth kinetics: insight into biomineralization. *Geochim. Cosmochim. Acta* **1999**, *63*, 2507–2512.
- (16) Falini, G.; Albeck, S.; Weiner, S.; Addadi, L. Control of aragonite or calcite polymorphism by mollusk shell macromolecules. *Science* **1996**, *271*, 67–69.
- (17) Belcher, A. M.; Wu, X. H.; Christensen, R. J.; Hansma, P. K.; Stucky, G. D.; Morse, D. E. Control of crystal phase switching and orientation by soluble mollusk-shell proteins. *Nature* **1996**, *381*, 56–58.
- (18) Mann, S. Molecular recognition in biomineralization. *Nature* **1988**, *332*, 119–124.
- (19) Hou, W. T.; Feng, Q. L. Crystal orientation preference and formation mechanism of nacreous layer in mussel. *J. Cryst. Growth* **2003**, *258*, 402–408.
- (20) Gower, L. A.; Tirrell, D. A. Calcium carbonate films and helices grown in solutions of poly(aspartate). *J. Cryst. Growth* **1998**, *91*, 153–160.
- (21) Falini, G. Crystallization of calcium carbonates in biologically inspired collagenous matrices. *Int. J. Inorg. Mater.* **2000**, *2*, 455–461.

CG0504861